LA-UR-23-32089

Approved for public release; distribution is unlimited.

Title:	GPS Energetic Charged Particle Data Product Files (v1.10)
Author(s):	Morley, Steven Karl Carver, Matthew Robert Hoover, Andrew Scott Merl, Robert Bernard
Intended for:	Documentation for dataset release Report
Issued:	2023-10-24

GPS Energetic Charged Particle Data Product Files (v1.10)

Steven K. Morley*, Matthew R. Carver†, Andrew S. Hoover‡, and Robert B. Merl§

Intelligence and Space Research (ISR) Division
Los Alamos National Laboratory

October 18, 2023

Copyright notice for the processed GPS data product files

Acknowledgement and citation request

If you use these data products, we would appreciate an acknowledgement of the source. The preferred acknowledgement is: "The CXD team at Los Alamos National Laboratory" rather than any individual's name. While the authors of this document are listed as points of contact if you have questions or comments about the data products, the CXD team is much larger. Because the historical GPS data products originate from instruments built and launched over a period of at least 25 years, the list of people who worked on the instruments is very long and has changed with time. The current members of the CXD team are listed at the end of this document. Some of the key papers describing the data set and some of the processing are referred to in this README and we ask that those most relevant to the user's application are cited. For the purposes of open science, we further request that when publishing work using these data products, or any derived products, the user provides a URL to the data holdings (hosted by NOAA's National Centers for Environmental Information) and information about the specific release number used.

*smorley@lanl.gov; ISR-1
†mrcarver@lanl.gov; ISR-1
‡ahoover@lanl.gov; ISR-1
§merl@lanl.gov; ISR-4

Version 1.10 release notes

This release improves on the previous dataset in several ways.

- The data are extended through April of 2023. See Figure 1 for a plot showing the temporal coverage for each satellite included in the release.
- A processing error was corrected that used incorrect proton responses in v1.09 (earlier versions were not affected). The primary impact was on Block IIF satellites.
- Constraints were placed on the parameters for the background term in the proton flux fits to mitigate rapid, unphysical changes in the fitted cosmic ray background.
- Some gaps in the previous data were recovered by using improved data processing tools.
- Additional handling of noisy channels has been added to the electron flux fit procedure to reduce fitting errors.
- A processing error was corrected that introduced incorrect differential fluxes in the BDD-IIR data files (ns41 and ns48); only the evaluated fluxes have changed, the fit coefficients were not affected.
- The cylindrical coordinates given by variables `b_coord_radius` and `b_coord_height` were erroneously reported in Geocentric Solar Magnetospheric (GSM) coordinates instead of Solar Magnetic (SM), this has been corrected.
- NOTE: No new on-orbit cross-calibration has been performed for, or using, the data taken after previously published on-orbit cross-calibration studies.

Please see section 2 for guidance on data caveats and usage.

1 Description of the contents of the data product files

The GPS Energetic Charged Particle data product files provide measurements, derived quantities, and modeled parameters for in situ radiation environment monitoring performed on the Global Positioning System constellation. The released data set contains energetic charged particle measurements from two different detector series: Burst Detection Dosimeter for Block II-R (BDD-IIR); and the Combined X-ray Dosimeter (CXD). The initial public release is described in [8] with some updates given by [2].

Instrument count rates are provided, however we also calculate an omnidirectional flux (normalized per steradian, per PRBEM standard guidelines). To obtain flux from the GPS energetic charged particle measurements we employ a forward modeling approach. We assume that the energy spectrum can be represented functionally and use a minimization approach to find the optimal values of the parameters for the functional form. The current data processing minimizes the negative log likelihood, minimizing the difference between the observed and expected count rates for the given forward model.

1.1 Instruments

The data products can be grouped by the detector series and the GPS block as shown in the table below. The BDD-IIR data are derived from BDD-IIR instruments on GPS Block IIR satellites and have fewer derived data products. The CXD data are derived from CXD instruments, which can be further identified by the block they are flown on. Although SVN74-75 are in GPS block III, the CXD instrument is of the IIF design. The CXD-IIR instruments on block IIR are identical to those on GPS IIR(M) satellites. The CXD instruments on SVN 76-79 are a CXD-III design and, as such, use new instrument responses to derive the fluxes. These have not been cross-calibrated on-orbit and should be used with care.

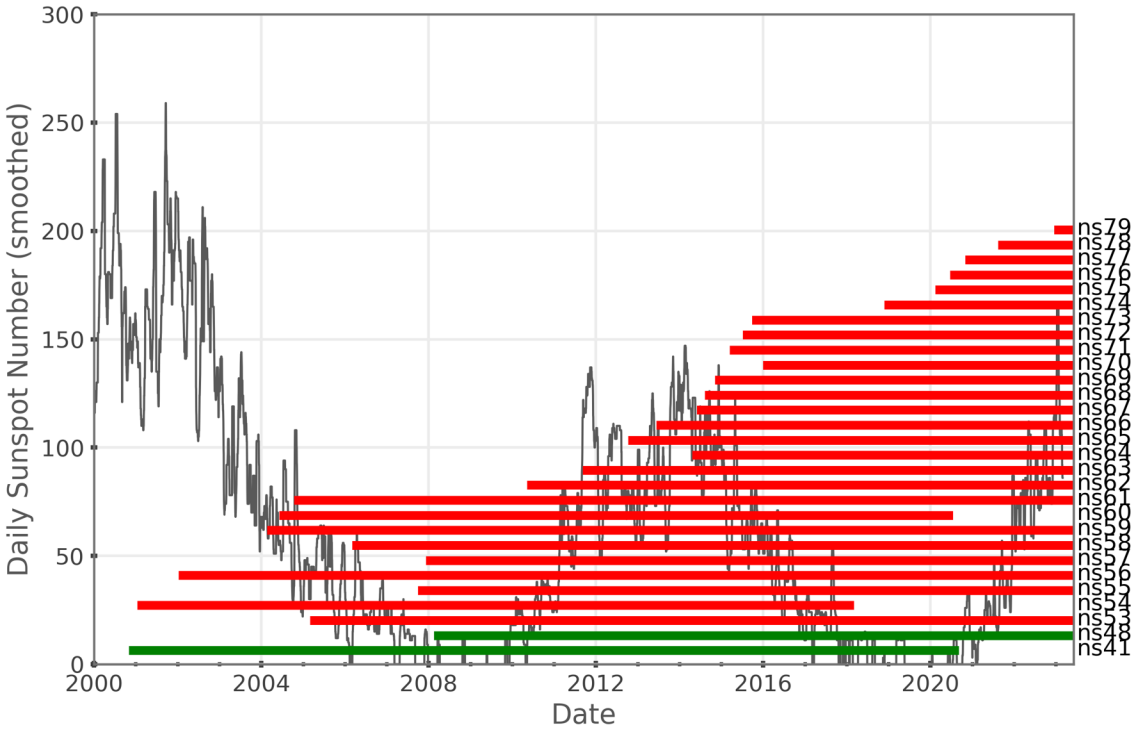

Figure 1: The temporal coverage of LANL/GPS energetic particle detectors included in the present data release. For solar cycle context we show the recalibrated daily sunspot number (from the Royal Observatory of Belgium) with the dark grey line. The data coverage for each satellite is shown by the horizontal bars, where different instrument packages have different colors and each bar is annotated with the satellite name. The red bars mark the coverage of CXD and the green bars mark the coverage of BDD-IIR.

SVN	Block	Instrument	Notes
41, 48	IIR	BDD-IIR	No proton flux, simple electron forward model, not cross-calibrated
53–61	IIR	CXD-IIR	53, 55, 57 & 58 are Block IIR(M)
62–73	IIF	CXD-IIF	
74–75	III	CXD-IIF	
76–79	III	CXD-III	

The BDD-IIR instruments are described in [13]. The lower energy dosimeter sensor in the CXD instruments is described in [14]. The cross-calibration of the CXD electron data with RBSP is described in [9], while the cross-calibration of CXD proton data with GOES is described in [3].

1.2 Data file contents

Each row in the data product files contains the data from one time bin from a CXD or BDD instrument along with a variety of products derived from the data. Integration time bin steps are commandable, but 4 minutes is a typical setting and is used across the vast majority of the data set. These instruments reside on many (but not all) GPS satellites that are currently in operation.

Each data product file contains data products from one GPS satellite for one GPS week. GPS weeks start at 00:00 each Sunday morning (GPS time). The times given in the data files, unless explicitly labeled, are given as GPS time. This scale differs from UTC due to the addition of leap seconds since the start of GPS time. GPS time and UTC coincide at 00:00 UTC on 6- Jan-1980 (at which time 9 leap seconds had been applied). Various software supports conversion between different time systems (e.g., GPS, UTC) including SpacePy[1] [10, 7].

1.2.1 Format and Metadata

The file name also contains the Space Vehicle Number (SVN), such that the individual satellites are interchangeably referred to as either SVN# or ns# (e.g., ns58 or SVN58). The data are provided as a self-describing ASCII format, where the metadata are provided in a header using JavaScript Object Notation (JSON). Each line in the header is prefixed with a #, so the header can be recognized and ignored if the metadata is not being used to parse the body of the file. The start column and number of columns for each variable are given in the metadata. The actual data are encoded as delimiter separated values (DSV). Specifically, these files use whitespace-delimited ASCII, which is compatible with many CSV (comma separated value) implementations. The JSON-headed ASCII format is also directly supported by software including SpacePy [10, 7] and Autoplot[2] [5].

The metadata supplied were originally designed to be compatible with the `QDataSet` model used by Autoplot [5]. Each variable has metadata that briefly describes the contents, the location(s) in the data file, and some metadata that can be used for automated visualization. The global metadata provides information about data file itself and its provenance. The table below provides an overview of the metadata variables used. Translations between the various space vehicle numbering schemes associated with each satellite can be found in a variety of places on the web, but we recommend using the tables given by [9, 8, 2].

Attribute name	Description
Global Metadata	
Copyright	Copyright statement for data product
Code_version_used	Indicates release version of the processing code
Data_origin	Source institution, instrument, SVN and creation date
ContactX	Contact details for named contact number X

[1] `https://github.com/spacepy/spacepy`
[2] `http://autoplot.org/`

Per-Variable Metadata	
DESCRIPTION	Textual description of variable
NAME	Variable name (e.g., column label in parser)
TITLE	Variable name used for automated title display
LABEL	Variable name (+units) used for automated axis labels
DIMENSION	Number of columns used by variable
UNITS	Units of stored variable
FILL_VALUE	Number used to indicate bad or missing data
ELEMENT_NAMES	Number of columns used by variable
ELEMENT_LABELS	Number of columns used by variable
START_COLUMN	Starting column for named variable (zero-based index)

1.2.2 Electron Data

The forward model for the BDD-IIR data is just a single Maxwell-Jüttner distribution (also known as the relativistic Maxwellian), and we obtain a temperature and number density through minimization. This function is given as:

$$j_{MJ}(E) = n\frac{c}{4\pi T K_2(\frac{m_e}{T})\exp(\frac{m_e}{T})}\frac{p^2}{m_e^2}\exp\left(\frac{E}{T}\right)\ [\mathrm{cm}^{-2}\mathrm{s}^{-1}\mathrm{MeV}^{-1}\mathrm{sr}^{-1}] \tag{1}$$

where n is the electron number density [cm^{-3}], E is the electron kinetic energy [MeV], p is the electron momentum [MeV/c], and m_e is the electron rest mass energy (0.51099891 MeV). K_2 is a modified Bessel function of the second kind (of order 2), and c is the speed of light, defined here as 2.998x10^{10} [cm/s].

For all CXDs (SVN $\geq$ 53), the electron data are also fit with a more complex functional form (see [9]) that is the sum of three Maxwell-Jüttner distributions (in energy) and a Gaussian (in log momentum). This functional form is flexible enough to represent typical energy spectra in the heart of the radiation belt and has been shown to provide a good representation of the spectrum [9]:

$$j_{CXD} = j_{MJ1}(n_1, T_1) + j_{MJ2}(n_2, T_2) + j_{MJ3}(n_3, T_3) + j_{Gauss}(n_G, \mu, \sigma) \tag{2}$$

where $j_{MJi}(n_i, T_i)$ are Maxwell-Jüttner functions as defined above, and

$$j_{Gauss} = n_G \exp\left(-\frac{\ln(P/\mu))^2}{2\sigma^2}\right) \tag{3}$$

The fitted fluxes are evaluated at a fixed set of energies and these are given in the data files (as variable `electron_diff_flux`). The fit parameters are also provided in the data files at each time step so that the fitted energy spectrum can be evaluated at any energy using the above formulae. The following table shows the correspondence between the fit parameters given in the variable `efitpars`.

Index	Variable	Description
1	n_1	Number density of MJ_1
2	T_1	Temperature of MJ_1
3	n_2	Number density of MJ_2
4	T_2	Temperature of MJ_2
5	n_3	Number density of MJ_3
6	T_3	Temperature of MJ_3
7	n_G	Number density of Gaussian
8	μ	Relativistic momentum at Gaussian peak
9	σ	Standard deviation of Gaussian

1.2.3 Proton Data

For the CXD data files only (SVN ≥ 53), the proton fluxes are obtained from a forward model that sums an exponential spectrum in momentum – which models solar energetic particle events – and a functional form to describe the cosmic ray background. The SEP spectrum is defined using:

$$j_{SEP} = \left[\frac{AN_0}{e^{43.33/r_0}}\right]\left(\frac{E}{p}\right)e^{-\frac{p}{r_0}} \tag{4}$$

where N_0 is the number density (obtained in the fit), p is the proton momentum (MeV/c), E is total proton energy (MeV), r_0 is the characteristic proton momentum (obtained in the fit), 43.33 represents the momentum of a proton with kinetic energy = 1 MeV, and $A = 0.046132$ is a normalization factor such that the flux is 1000 protons / (cm^2 sec sr MeV) at 1 MeV of kinetic energy.

$$j_{bkg} = B\left[j_1 + f(j_2 - j_1)\right] \tag{5}$$

where the fit parameters B and f are an overall normalization and f is a value between 0 and 1 representing some intermediate form between j_1 and j_2 (representing solar minimum and maximum, respectively), which are defined in equation 6. As of release 1.10, B is constrained to lie in the range [0.5, 2].

$$j_n = A_n \exp\left[\frac{-\left[\log\frac{E}{E_{0n}}\right]^2}{2\sigma_n}\right] + B_n E^{-C_n} \tag{6}$$

where the five parameters with the n subscript are a 5 parameter fit to the CREME96 simulation of the galactic cosmic ray background at solar minimum (1) and maximum (2) at GPS altitude with values given in the table below. See [3] and references therein for details of this proton flux forward model.

Parameter	A	E_0	σ	B	C
Solar Min.	$1.076\text{x}10^{-4}$	$3.293\text{x}10^{2}$	1.305	2.441	$3.671\text{x}10^{-2}$
Solar Max.	$3.286\text{x}10^{-5}$	$7.463\text{x}10^{2}$	1.202	2.887	$2.467\text{x}10^{-2}$

1.2.4 Additional quantities

Remaining quantities in the data product files are described in the table below. The magnetic field dependent quantities are calculated using the LANLGeoMag library [6].

Variable name	type	Dim.	description
decimal_day	double	1	Fractional day, GPS time. A number from 1 (1-Jan 00:00) to 366 (31-Dec 24:00) or 367 in leap years.
Geographic_Latitude	double	1	Geocentric geographic latitude of satellite (deg)
Geographic_Longitude	double	1	Geocentric geographic longitude of satellite (deg)
Rad_Re	double	1	Radius (i.e., magnitude of position vector) in Earth radii
rate_electron_measured	double	11	Measured count rate (Hz) in each of the 11 CXD electron channels
rate_proton_measured	double	5	Measured count rate (Hz) in each of the 5 CXD proton channels (P1-P5)
LEP_thresh	double	1	LEP threshold in E1 channels (0 means low, 1 means high)
collection_interval	double	1	dosimeter collection period (seconds)
year	int	1	year (e.g. 2015)
decimal_year	double	1	decimal year = year + (decimal_day-1.0)/(days in year)
svn_number	int	1	SVN number of satellite
dropped_data	int	1	if =1 it means something is wrong with the data record, do not use it
b_coord_radius	double	1	radius from Earth's dipole axis (Earth radii)

b_coord_height	double	1	height above the Earth's dipole equatorial plane (Earth radii)
magnetic_longitude	double	1	Magnetic longitude (degrees)
L_shell	double	1	L_shell (Earth radii) – currently this is the same as L_LGM_T89IGRF. Which field models this uses may change in a future release.
L_LGM_TS04IGRF	double	1	LANLGeoMag McIlwain L calculation, TS04 External Field, IGRF Internal Field.
L_LGM_OP77IGRF	double	1	LANLGeoMag McIlwain L calculation, OP77 External Field, IGRF Internal Field
L_LGM_T89CDIP	double	1	LANLGeoMag McIlwain L calculation, T89 External Field, Centered Dipole Internal Field
L_LGM_T89IGRF	double	1	LANLGeoMag McIlwain L calculation, T89 External Field, IGRF Internal Field
bfield_ratio	double	1	Bsatellite/Bequator
local_time	double	1	magnetic local time (0-24 hours)
utc_lgm	double	1	Fractional day, UTC (0-24 hours)
b_satellite	double	1	B field at satellite (Gauss)
b_equator	double	1	B field at equator (on this field line) (Gauss)
istat_Lgm	int	1	Flag indicating input data quality used in LANLGeoMag magnetic field model calculations. 0 is definitive data, 1 is defaults used. -1 is fill (variable not currently used).
electron_background	double	11	estimated background count rate in electron channels E1-E11 (Hz)
proton_background	double	5	estimated background count rate in proton channels P1-P5 (Hz)
proton_activity	int	1	=1 if there is significant proton activity
proton_temperature_fit	double	1	characteristic momentum – R0 in the expression given above (MeV/c)
proton_density_fit	double	1	proton number density fit (cm-3)
electron_temperature_fit	double	1	electron temperature from an initial relativisticMaxwellian fit (MeV)
electron_density_fit	double	1	electron number density fit (cm-3)
model_counts_electron_fit_pf	double	11	E1-E11 count rates due to proton background
			based on proton flux fit
model_counts_proton_fit_pf	double	5	P1-P5 count rate evaluated from proton fit (using
			proton_temperature_fit, proton_density_fit)
model_counts_electron_fit	double	11	E1-E11 count rates evaluated from the 9- parameter electron flux forward model
model_counts_proton_fit	double	5	P1-P5 count rates evaluated from forward model – currently not filled (all -1's)
proton_integrated_flux_fit	double	6	integral of proton flux (based on fit) above 10, 20, 30, 50, 60, and 100 MeV (proton kinetic energy) [$cm^{-2}sec^{-1}sr^{-1}$]
proton_flux_fit	double	31	Differential proton flux at 31 energies [$cm^{-2}sec^{-1}sr^{-1}MeV^{-1}$]
proton_flux_fit_energy	double	31	energies for the fluxes in proton_flux_fit [MeV]
proton_fluence_fit	double	6	integral proton fluence at the six energies of the proton_integrated_flux_fit above (cm-2sr-1)
integral_flux_instrument	double	30	(based on 9 parameter fit) integral of electron flux
			above integral_flux_energy[i] particles/(cm2 sec)
integral_flux_energy	double	30	energies for the integral of integral_flux_instrument (MeV)
electron_diff_flux_energy	double	15	energies for the fluxes in electron_diff_flux_energy (MeV)

electron_diff_flux	double	15	(based on 9 parameter fit) electron flux at energies electron_diff_flux[i] (particle/(cm2 sr MeV sec))
efitpars	double	9	Fit parameters for 9 parameter electron fit
pfitpars	double	4	Fit parameters for 4 parameter proton fit.

SVN41 and 48 have slightly different data products, differences are as described in the following table.

Variable name	type	Dim.	Description
L_shell	double	1	L_shell – dipole field/T-89
diffp	double	1	No longer used
sigmap	double	1	No longer used
electron_background	double	8	estimated background in electron channels E1-E8 (Hz)
proton_background	double	8	estimated background in proton channels P1-P8 (Hz)
model_counts_electron_fit	double	8	E1-E8 rates from the 2-parameter Maxwellian fit to the electron data
dtc_counts_electron	double	8	Dead time corrected electron rates (from data, not fit)
electron_diff_flux_energy	double	15	energies for the fluxes in electron_diff_flux_energy (MeV)
electron_diff_flux	double	15	(based on 2-parameter relativistic Maxwellian fit) electron flux at energies electron_diff_flux[i] (particle/(cm^2 sr MeV sec))

2 Data Usage and Caveats

The CXD and BDD-IIR data products have limitations. We document key known limitations here, with potential mitigation.

- All data products are fits that use a forward model. These forward models are described in sections 1.2.2 and 1.2.3, and thus presented fluxes are *evaluated* and are *not* channel fluxes. The derived fluxes are generally reliable and well-calibrated [9, 3, 4], but this is subject to the fits converging and fit quality should be taken into account.
- Fit quality flags are currently being developed and tested. For CXD electron flux a conservative way to filter out suspect fits is presented by [12]: $F = \max\left(\frac{\hat{R}}{R}\right)$, where $F > 0.11$ are deemed to be low quality fits (noting that this is focused on sub-MeV energies). This will also often reject good fits at times of low flux. Note that some SVNs consistently have poorer fits (e.g., ns60 and ns69) by this measure and should be inspected before use.
- The CXD electron forward model includes 3 Maxwell-Jüttner components with different characteristic temperatures. The highest temperature of these can often present as a fit to background as > 4 MeV flux is infrequently high enough for CXD to measure. This effect is reduced in this data release, but energies above 3-4 MeV should be inspected before use.
- The CXD proton fluxes are calculated using a forward model including a reduced-parameter version of the CREME96 GCR model as a background component. This model shows a strong increasing trend in flux at low energy, contrary to other, more recent, GCR models. Work is ongoing to update the forward model, but the background fit should not be taken as a meaningful measure of GCR flux.
- The CXD proton flux forward model does not include geomagnetic shielding. While the calculated fluxes have been shown to capture geomagnetic shielding to some degree [4, 15], the spectral model does not support a low-energy/rigidity cutoff. The calculated flux spectra at low-L are unlikely to be valid.
- The CXD P3 proton channel is known to have a response to relativistic electrons. This can be noticeable at lower L during strong radiation belt enhancements. As such the proton flux spectra at these times should be considered unreliable.

- The magnetic field-dependent quantities (L, SM cylindrical coordinates, magnetic field strength at satellite, magnetic field ratio, ...) are all calculated using magnetic field models implemented in the LANLGeoMag software library [6]. The default field model (unless otherwise specified) is currently the Tsyganenko 1989c [11] as the external field, with the internal field given by the IGRF [1].
- Satellites launched after the on-orbit cross-calibration papers (and the events used in them) have not been subject to a quantitative on-orbit cross-calibration. This work is pending and, while broad consistency has been checked, the data should be use with care.

3 Current members of the CXD team

In alphabetical order of surname:

Alex Adams, Steven Armijo, Elizabeth Auden, Scott Barcus, Darrel Beckman, Kerry Gardiner Boyd, Michael Caffrey, Matthew Carver, Yue Chen, Stephen Craft, Alejandro Cruz Gonzalez, Cordell Delzer, Jonathan Deming (Chief Engineer), Robert Dingler, James Distel, Trent English, Tatiana Espinoza, Adam Esquibel, Thomas Fairbanks, Christopher Franco, Orlando Garduno, Katherine Gattiker, Jeffrey George, Ryan Hemphill, Samuel Henderson, Michael Holloway, Andrew Hoover (Chief Scientist), Felix Liang, Roger Lujan, Ramona Maestas, Nathan Martin, Susan Mendel, Robert Merl (Project Leader), Rod Mesecar, Zachary Bryan Miller, Joshua Camen Montoya, Steve Morley, Ben Norman, Doug Patrick, Dan Poulson, Ethan Randall, Craig Reingold, Grant Riley, Tony Rogers, Penny Salazar, Rudy Salazar III, Marcus Sanders, Gina Sandoval, Noah Schmidt, Brayden Stidham, Jon Teague, Melinda Vigil, Howard Watson.

References

[1] P. Alken, E. Thébault, C. D. Beggan, H. Amit, J. Aubert, J. Baerenzung, T. Bondar, W. Brown, S. Califf, A. Chambodut, et al. International geomagnetic reference field: the thirteenth generation. *Earth, Planets and Space*, 73(1):1–25, 2021. https://doi.org/10.1186/s40623-020-01288-x.

[2] M. Carver, S. K. Morley, and A. Stricklan. GPS constellation energetic particle measurements. In *2020 IEEE Aerospace Conference*, pages 1–10, 2020. https://doi.org/10.1109/AERO47225.2020.9172652.

[3] M. R. Carver, J. P. Sullivan, S. K. Morley, and J. V. Rodriguez. Cross calibration of the GPS constellation CXD proton data with GOES EPS. *Space Weather*, 16(3):273–288, 2018. https://doi.org/10.1002/2017SW001750.

[4] Y. Chen, S. K. Morley, and M. R. Carver. Global prompt proton sensor network: Monitoring solar energetic protons based on GPS satellite constellation. *Journal of Geophysical Research: Space Physics*, 125(3):e2019JA027679, 2020. https://doi.org/10.1029/2019JA027679.

[5] J. B. Faden, R. S. Weigel, J. Merka, and R. H. W. Friedel. Autoplot: a browser for scientific data on the web. *Earth Science Informatics*, 3:41–49, 2010. https://doi.org/10.1007/s12145-010-0049-0.

[6] M. Henderson, S. Morley, J. Niehof, and B. Larsen. drsteve/LANLGeoMag: LANLGeoMag v.1.5.16. Mar 2018. https://dx.doi.org/10.5281/zenodo.1133781 and https://github.com/drsteve/LANLGeoMag.

[7] S. K. Morley, J. T. Niehof, D. T. Welling, B. A. Larsen, A. Brunet, M. A. Engel, J. Gieseler, J. Haiducek, M. Henderson, A. Hendry, M. Hirsch, P. Killick, J. Koller, A. Merrill, A. Reimer, A. Y. Shih, and A. Stricklan. SpacePy, Sept. 2022. https://doi.org/10.5281/zenodo.7083375.

[8] S. K. Morley, J. P. Sullivan, M. R. Carver, R. M. Kippen, R. H. W. Friedel, G. D. Reeves, and M. G. Henderson. Energetic Particle Data From the Global Positioning System Constellation. *Space Weather*, 15(2):283–289, 2017. https://doi.org/10.1002/2017sw001604.

[9] S. K. Morley, J. P. Sullivan, M. G. Henderson, J. B. Blake, and D. N. Baker. The Global Positioning System constellation as a space weather monitor: Comparison of electron measurements with Van Allen Probes data. *Space Weather*, 14(2):76–92, 2016. https://doi.org/10.1002/2015SW001339.

[10] J. T. Niehof, S. K. Morley, D. T. Welling, and B. A. Larsen. The SpacePy space science package at 12 years. *Frontiers in Astronomy and Space Sciences*, 9, 2022. https://doi.org/10.3389/fspas.2022.1023612.

[11] M. Peredo, D. P. Stern, and N. A. Tsyganenko. Are existing magnetospheric models excessively stretched? *Journal of Geophysical Research: Space Physics*, 98(A9):15343–15354, 1993. https://doi.org/10.1029/93JA01150.

[12] A. G. Smirnov, M. Berrendorf, Y. Y. Shprits, E. A. Kronberg, H. J. Allison, N. A. Aseev, I. S. Zhelavskaya, S. K. Morley, G. D. Reeves, M. R. Carver, and F. Effenberger. Medium Energy Electron Flux in Earth's Outer Radiation Belt (MERLIN): A Machine Learning Model. *Space Weather*, 18(11):e2020SW002532, 2020. https://doi.org/10.1029/2020SW002532.

[13] M. Tuszewski, T. Cayton, and J. Ingraham. A new numerical technique to design satellite energetic electron detectors. *Nuclear Instruments and Methods in Physics Research Section A: Accelerators, Spectrometers, Detectors and Associated Equipment*, 482(3):653–666, 2002. https://doi.org/10.1016/S0168-9002(01)01735-1.

[14] M. Tuszewski, T. E. Cayton, J. C. Ingraham, and R. M. Kippen. Bremsstrahlung effects in energetic particle detectors. *Space Weather*, 2(10), 2004. https://doi.org/10.1029/2003SW000057.

[15] C. M. van Hazendonk, E. Heino, P. T. A. Jiggens, M. G. G. T. Taylor, N. Partamies, and H. C. J. Mulders. Cutoff latitudes of solar proton events measured by GPS satellites. *Journal of Geophysical Research: Space Physics*, 127(3):e2021JA030166, 2022. https://doi.org/10.1029/2021JA030166.